

Minimizing Grating Lobes in Large Arrays Using Clustered Amplitude Tapers

Jafar Ramadhan Mohammed*

Abstract—One of the common ways to design large arrays is by designing a small subarray known as cluster and using it as a repeating element throughout a large array. In this paper, the genetic algorithm is used to optimize the clustered amplitude tapers such that the final array pattern has minimum grating lobes and controlled sidelobe level. The formulation of the synthesis problem includes the minimization of the excess magnitude of the grating lobes or peak sidelobes which are usually higher than a given allowable limit. Moreover, two clustered configurations based on increased/decreased number of elements per cluster around the array center are introduced. Correspondingly, their clustered sizes increase/decrease as they approach the center of the array. Simulation results show that the proposed method has capability to optimize clustered linear and planar arrays without noticeable appearance of undesirable grating lobes. The analysis for an array composed of 20 elements with clusters of different cluster sizes $M = 10, 8, 5, 4$ and different numbers of elements per cluster $N_s = 2, 3, 4, 5$ found that the complexity reductions were 50%, 60%, 75%, 80%; peak sidelobe levels were -29 dB, -23.6 dB, -21.3 dB, -19.15 dB; and the directivities were 25.53 dB, 25.64 dB, 26.33 dB, 26.32 dB, respectively.

1. INTRODUCTION

The performance of the antenna arrays increases steadily to an increase in the number of deployed elements. These improvements come at the cost of larger arrays, higher manufacturing costs, and more complex feeding network circuitry [1]. Intuitively, smaller aperture array sizes can be obtained by reducing the interelement spacing which will not be a good option in practice due to many limitations such as mutual coupling between neighboring elements which surely causes significant degradation in the overall array performance [2, 3].

One of the efficient methods for building large arrays is to design a small subarray and use it as a repeating element throughout a large array. In this case, the excitation amplitudes and phases at both element level and subarray level need to be carefully determined to meet the required radiation pattern and at the same time to avoid undesirable grating lobes [4, 5]. In the literature, many researchers have pointed out that the portioned array into regularly spaced smaller subarrays introduces grating lobes and causes high sidelobes in its radiation pattern [6, 7]. To avoid these effects, irregular subarrays were proposed in [8] where a random trial and error method was used to partition a circular planar array to produce a difference pattern with low sidelobes. However, it is found that such a configuration did not provide the required low sidelobe sum pattern.

The authors in [9] showed that each subarray in the partitioned array must be unique in shape (i.e., random) to reduce the undesirable effects. Later, the authors in [10–13] suggested the use of regularly shaped building blocks that are randomly combined to create an irregular set of subarray phase centers. The best way for combining these building blocks perfectly and optimally determining their excitation weights is to use an optimization algorithm. The early work by [14] used genetic

Received 17 March 2022, Accepted 26 April 2022, Scheduled 7 May 2022

* Corresponding author: Jafar Ramadhan Mohammed (jafarram@yahoo.com).

The author is with the College of Electronics Engineering, Nineveh University, Mosul 41002, Iraq.

algorithm to optimize the amplitude tapers of the subarray in the linear and planar arrays, but the subarray shape was not subject to optimization. The GA was also used by [15–17] to optimize thinned linear arrays. Rodriguez et al. [18] used simulated annealing to configure between two different radiation patterns by optimizing a number of parameters in a combined fitness function in subarrayed linear and planar antennas. Lopez and Rodriguez [19] used a simple divider method based on genetic algorithm to optimize both the number of elements in each subarray and subarray weights in linear arrays. The authors in [13, 20] proposed two different architectures based on fully and partially clustered arrays to achieve the required array patterns. In the fully clustered arrays, all the elements of the original array were divided into several equal subarrays, while in the partially clustered arrays, only the side elements were grouped into subarrays, and the central elements were left individually.

In this paper, the method presented in [13] is further extended to planar arrays to deal with the problem of grating lobes by formulating different clustered configurations. Moreover, two new irregular clustered configurations based on either increased or decreased number of elements per successive clusters are introduced. In each configuration, the clustered amplitude tapers are optimized such that the grating lobes and side lobes are both simultaneously minimized. These clustered configurations lead to a better design in terms of simple feeding network and save significant time in the synthesis of large antenna arrays.

2. SUBARRAYS AND PROBLEM FORMULATION

It is well known that the overall array pattern (AP) of an ordinary linear array with N individual radiating elements (i.e., without any subarrays) can be given by [21]:

$$AP(\theta) = \sum_{n=1}^N \underbrace{EP_n(\theta)}_{\text{Elemental Pattern}} \underbrace{a_n e^{jp_n} e^{j(n-1)kd \sin(\theta)}}_{\text{Array Factor}} \quad (1)$$

It is clear from Eq. (1) that the overall array pattern is the multiplication of the elemental pattern, $EP_n(\theta)$, and the array factor determined by the inter-element spacing, d , excitation amplitude, a_n , and phase, p_n of the n th element. Note that for isotropic elements all the $EP_n(\theta)$ terms will be identical. The other variables are defined as $k = \frac{2\pi}{\lambda}$; λ is the wavelength; and θ is the observation angle normal to the array.

On the other hand, when using subarrays as elements instead of Eq. (1), then the final array pattern, AP , is the multiplication of the elemental pattern, the AF of subarray, and the AF of the fullarray determined by the spacing, amplitude, and phasing between individual subarrays as follows:

$$AP(\theta) = EP(\theta) \times AF_{\text{subarray}}(\theta) \times AF_{\text{fullarray}}(\theta) \quad (2)$$

$AF_{\text{fullarray}}$ with a number of subarrays equal to M can be written as

$$AF_{\text{fullarray}}(\theta) = \sum_{m=1}^M b_m \sum_{n=1}^{N_s} \underbrace{a_{mn} e^{jk[d_{(m-1)N_s+n}] \sin(\theta)}}_{\text{Subarray as Elements}} \quad (3)$$

where b_m is the excitation amplitude at the m th subarray; N_s is the total number of elements per subarray; a_{mn} is the excitation amplitude at the n th element and m th subarray; and $d_{(m-1)N_s+n}$ is the distances of the elements from the array center.

From Eq. (2), it can be seen that there are three different levels, namely, element level, subarray level where the individual elements are arranged in a subarray, and the fullarray level where subarrays act as elements. The final $AP(\theta)$ according to Eq. (2) combines these three patterns and may show high sidelobe levels or even grating lobes in its final pattern. The grating lobes and high sidelobe levels usually appear in the fullarray level as a result of uniformly spaced smaller subarrays. Fig. 1 shows the array patterns determined according to Eqs. (2) and (3) and its subarray configuration for used parameters; $M = 10$, $N_s = 2$, $b_m = 1$, $a_{mn} = 1$, $d = 0.5\lambda$. From this figure, it can be seen that, under the assumption of uniform excitation, the exact matching among all grating lobes peaks of the fullarray pattern and the nulls of the subarray pattern is feasible. Thus, cancellation of grating lobes after pattern multiplication was noticed; however, high SLL is still noticed. Minimizing both the grating lobes and the peak SLL are presented in the next section.

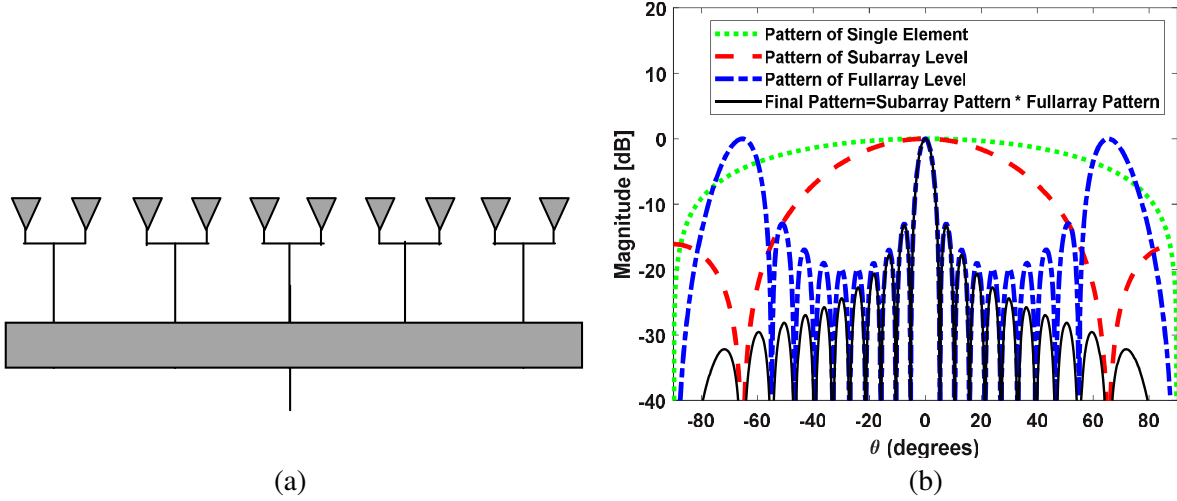


Figure 1. Principles of subarray for $E = 20$, $M = 10$, and $N_s = 2$. (a) Array configuration and (b) array patterns.

3. DESCRIPTION OF THE METHOD

In this section, the array elements are portioned into smaller subarrays known as clusters. Different cluster shapes and sizes ranging from small to large size clusters are considered, and their clustered amplitude tapers are optimized to get the required array patterns with minimized grating lobes and sidelobes. For linear arrays, the method starts by dividing the total number of linear array elements, $E = N_s \times M$ into M clusters and N_s elements per cluster. Note that the total number of array elements, E , does not have to be an integer multiple of the subarray elements where in some cases the clusters at the end of the array may have fewer elements per cluster than those of the nearest clusters to the array center which leads to an irregular clusters configuration. As an example, the configurations shown in Fig. 2 have $E = 20$, $M = 10, 8, 4$ and $N_s = 2, 3, 5$, respectively. Note that for $M = 8$, the possible number of elements per cluster is 1, 3, 3, 3, 3, 3, 3, 1. The array is assumed to be symmetric about its physical center, thus, only half of the array elements and their corresponding clusters are pictured in the above mentioned figure.

The final array pattern for such a linear clustered array is given by

$$AP_{cluster}(\theta) = \sum_{m=1}^M b_m \sum_{n=1}^{N_s} a_{mn} \cos[k(x_m + x_n) \sin \theta] \quad (4)$$

where $x_n = (n-1)d$ is the inter-element spacing at the element level, while x_m is the inter-cluster spacing at the cluster level. b_m and a_{mn} are the optimization variables for obtaining the desired array pattern. Here, a_{mn} are set to unity whereas the variables b_m are optimized. Thus, the genetic algorithm (GA) has only M parameters to optimize. A genetic algorithm with an allowable constraint on the sidelobe level is needed as follows. The normalized constraint mask, in decibels, can be written as:

$$Mask(\theta) = \begin{cases} SLL, & -90^\circ \leq \theta \leq -FNBW, FNBW \leq \theta \leq 90^\circ \\ 0, & -FNBW \leq \theta \leq FNBW \end{cases} \quad (5)$$

where $FNBW$ is the first null to null beam width of the array pattern, and SLL is the allowable sidelobe level. The cost function that is used to optimize the b_m under the above mentioned constraint mask can be written as:

$$Cost = \sum_{p=1}^P |AP_{cluster}(\theta_p) - Mask(\theta_p)|^2 \quad (6)$$

where $p = 1, 2, \dots, P$ are the considered sample points. Note that the cost will minimize any excess magnitudes of the $AP_{cluster}(\theta_p)$ located outside the allowable SLL which in turn minimizes both the grating lobes and sidelobes. The cost function will force the optimizer to adjust the weights, b_m , to set the sidelobes of the clustered array as close as possible to the mask limit.

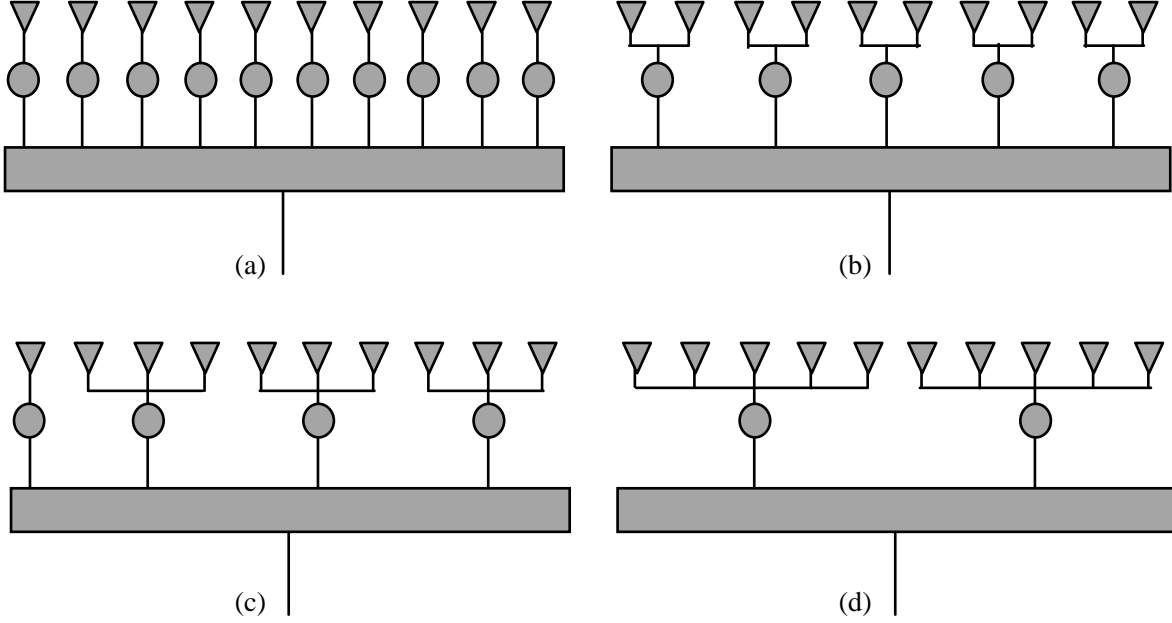


Figure 2. Different array configurations for $E = 20$. (a) Normal array, (b) $M = 10$ and $N_s = 2$, (c) $M = 8$ and $N_s = 3$, (d) $M = 4$ and $N_s = 5$.

For the two dimensional clustered rectangular planar arrays, first recall the space variables u and v which can be defined as functions of the elevation angle θ and the azimuth angle ϕ by $u = \sin \theta \cos \phi$ and $v = \sin \theta \sin \phi$. Consequently, these variables at the element and clustered levels will be represented by u_e, v_e and u_c, v_c , respectively. Note that the rectangular planar array has been formed by simply multiplying two linear arrays on the x and y axes such that it has $E_x \times E_y$ elements distributed along the xy plane with inter-element spacing d_{xe}, d_{ye} and inter-cluster spacing d_{xc}, d_{yc} , respectively.

$$AP_{cluster}(u, v) = \sum_{m_x=1}^{M_x} \sum_{m_y=1}^{M_y} b_{m_x m_y} \cos[(m_y - 0.5) \psi_{yc}] \cos[(m_x - 0.5) \psi_{xc}] \sum_{n_x=1}^{N_x} \sum_{n_y=1}^{N_y} a_{n_x n_y} \cos[(n_y - 0.5) \psi_{ye}] \cos[(n_x - 0.5) \psi_{xe}] \quad (7)$$

where $\psi_{xe} = kd_{xe}u_e$, $\psi_{ye} = kd_{ye}v_e$, $\psi_{xc} = kd_{xc}u_c$, and $\psi_{yc} = kd_{yc}v_c$. Again the cost function in Eq. (6) is used to minimize the grating lobes according to the given mask constraints.

4. SIMULATION RESULTS

In the following, all the presented examples are based on the linear and planar antenna arrays with interelement spacing $d = 0.5\lambda$, and the optimization parameters were: an initial population size is 50; number of iterations is set to 1000; selection is roulette; number of crossovers is 2; mutation probability is 0.04; and mating pool is chosen to be 4. The minimum and maximum values of the excitation amplitudes are bounded between $0 \sim 1$, and the excitation phases were fixed to zeros. The mask sidelobe level for all considered examples was set to -30 dB.

In the first example, many cluster sizes with different numbers of elements per cluster were considered to study the variations in the array performance in terms of complexity reduction, directivity, peak SLL, average SLL, half power beam width (HPBW), and the taper efficiency. The complexity reduction was defined by the ratio of the number of clusters to the total number of array elements, while the average SLL was defined as the total area under the sidelobes pattern. Table 1 illustrates all the above mentioned variations under different cluster sizes and number of elements per cluster. This table also shows the optimized values of the clustered amplitude tapers (due to symmetrical array, only half values of the array elements were shown). Fig. 3, Fig. 4, Fig. 5, and Fig. 6 show the results for

Table 1. Array performances versus cluster sizes for $E = 20$ linear array elements.

Performances	Fully Optimized Array	Clustered Array									
		No. of Elements per Cluster									
		1	2	3	4	5	6	7	8	9	10
		No. of Cluster's Weight									
		20	10	8	5	4	5	8	6	4	2
Complexity Reduction	0%	0%	50%	60%	75%	80%	75%	60%	70%	80%	100%
Taper Efficiency	0.73	0.77	0.86	0.84	0.91	0.91	0.91	0.83	0.86	0.94	1
Directivity (dB)	24.85	25.17	25.53	25.64	26.33	26.32	26.39	25.57	25.84	26.58	27.16
Peak SLL (dB)	-30	-30	-29	-23.6	-21.3	-19.1	-15	-15	-13.8	-13.2	-13.2
Average SLL (dB)	-22.6	-23.1	-23.0	-21.8	-21.5	-21.3	-20.2	-20.7	-20.1	-20.4	-20.2
HPBW (deg.)	7.11	6.84	6.17	6.44	5.90	5.86	5.68	6.35	6.04	5.50	5.50
	Fully Array Weights	Subarray Weights									
Excitation Amplitudes	0.13	0.13	0.19	0.18	0.48	0.52	0.09	0.15	0.09	0.21	1.00
	0.19	0.19	0.19	0.35	0.48	0.52	0.88	0.20	0.24	1.00	1.00
	0.37	0.37	0.48	0.35	0.48	0.52	0.88	0.44	1.00	1.00	1.00
	0.48	0.48	0.48	0.35	0.48	0.52	0.88	1.00	1.00	1.00	1.00
	0.52	0.52	0.73	0.81	0.96	0.52	0.88	1.00	1.00	1.00	1.00
	0.73	0.73	0.73	0.81	0.96	1.00	0.88	1.00	1.00	1.00	1.00
	0.78	0.78	0.94	0.81	0.96	1.00	0.88	1.00	1.00	1.00	1.00
	0.94	0.94	0.94	1.00	0.96	1.00	1.00	1.00	1.00	1.00	1.00
	0.98	0.98	1.00								
	1.00	1.00	1.00	1.00	1.00	1.00	1.00	1.00	1.00	1.00	1.00

$E = 20$ elements, $M = 10, 8, 5, 4$ clusters, and $N_s = 2, 3, 4, 5$ elements per cluster, respectively. The clusters configurations of these four cases were previously shown in Fig. 2. From this table and these figures, it can be seen that when the number of clusters is increased, the complexity reduction increases, and both the taper efficiency and the directivity are improved, while the peak SLL and average SLL are decreased. Fig. 3 confirms that the two array patterns of the fully optimized array elements and the proposed clustered array with $M = 10$ clusters, and $N_s = 2$ are largely indistinguishable, and both patterns obey the allowable constraint mask.

In the second example, the cluster size was gradually increased by increasing its number of elements until approaching the center of the array. In other words, the first cluster which is the farthest one contains only a single element, and the second one contains 2 elements per cluster, while the third one contains 3 elements per cluster and so on. Fig. 7 shows the proposed clustered array configuration and its results, while Table 2 shows its performance measures. From these results, it can be found that the peak SLL of this case is -25 dB, and the two desired wide nulls centered at $\pm 35^\circ$ are accurately placed.

In the next example, the cluster size was gradually decreased by decreasing its number of elements

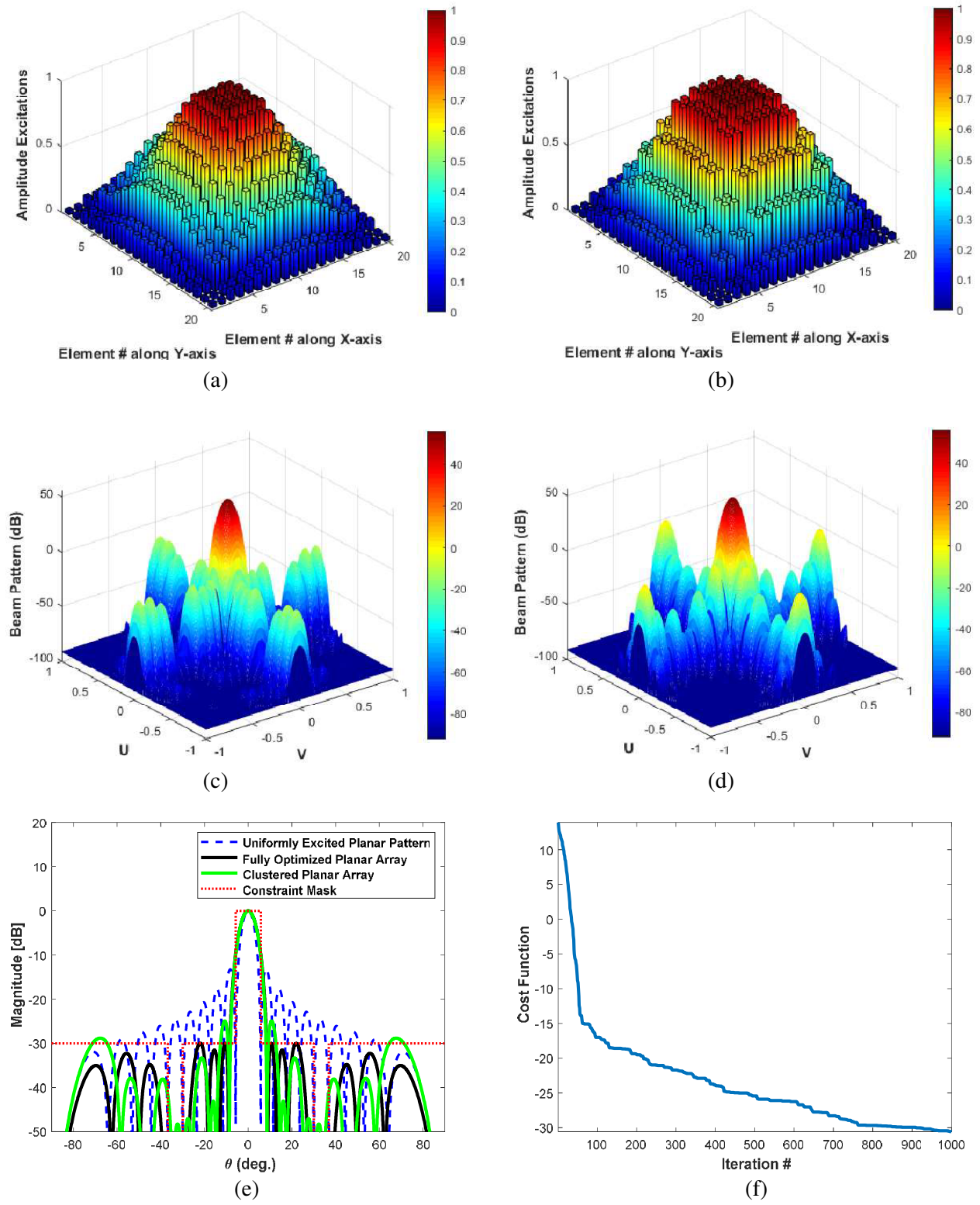


Figure 3. The results for $E = 20$, $M = 10$ and $N_s = 2$. (a) Amplitude taper of fully optimized array, (b) amplitude taper of clustered array, (c) fully optimized array pattern, (d) clustered array pattern, (e) 2D array patterns, and (f) cost function variations.

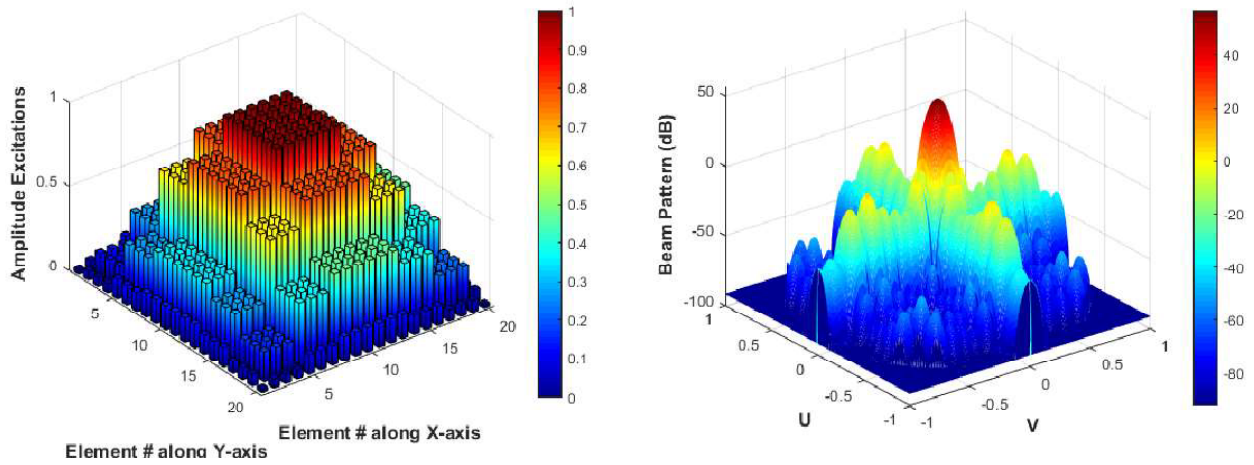


Figure 4. The results for $E = 20$, $M = 8$ and $N_s = 3$. The peak sidelobe level is -23.6 dB.

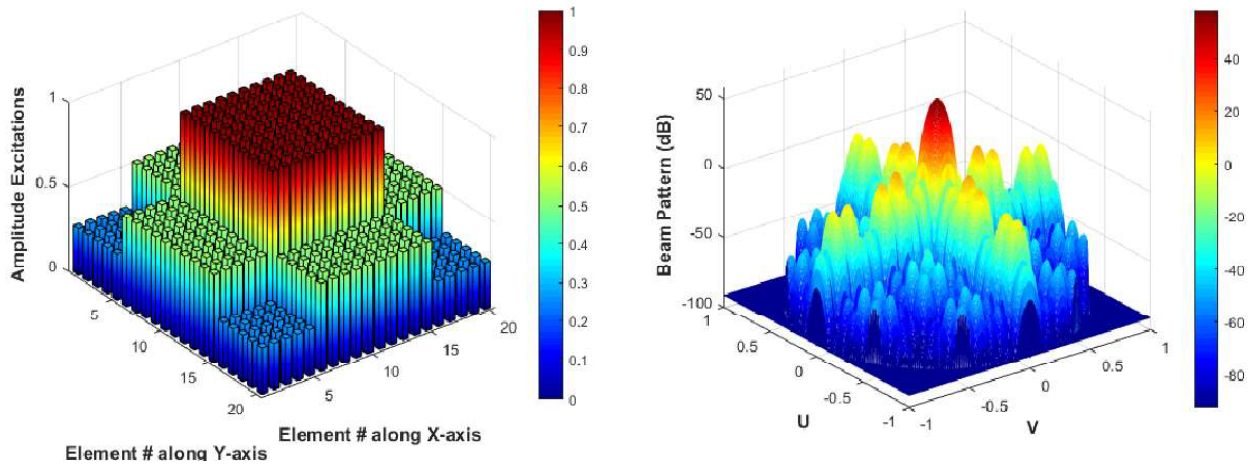


Figure 5. The results for $E = 20$, $M = 4$ and $N_s = 5$. The peak sidelobe level is -19.15 dB.

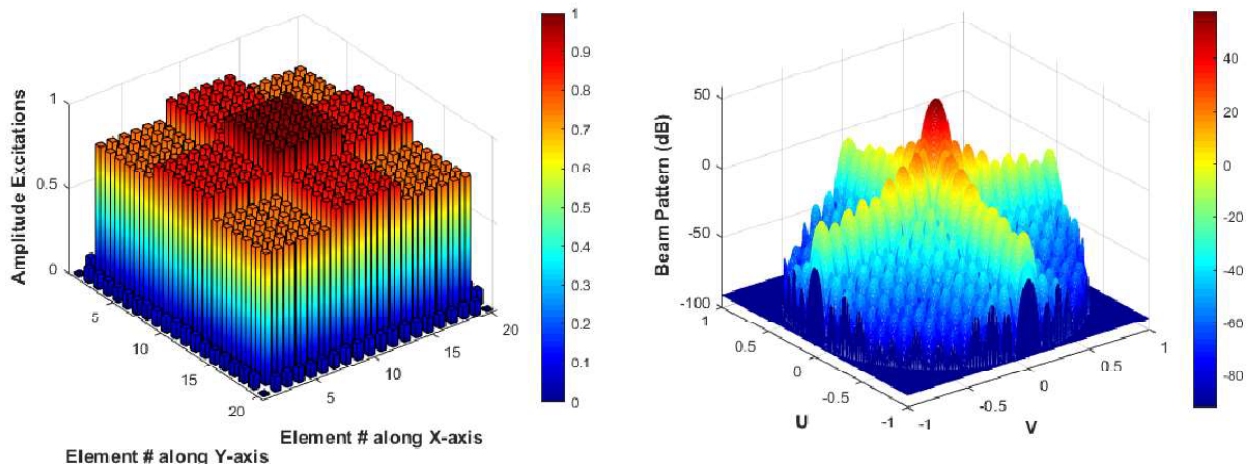


Figure 6. The results for $E = 20$, $M = 5$ and $N_s = 6$. The peak sidelobe level is -15 dB.

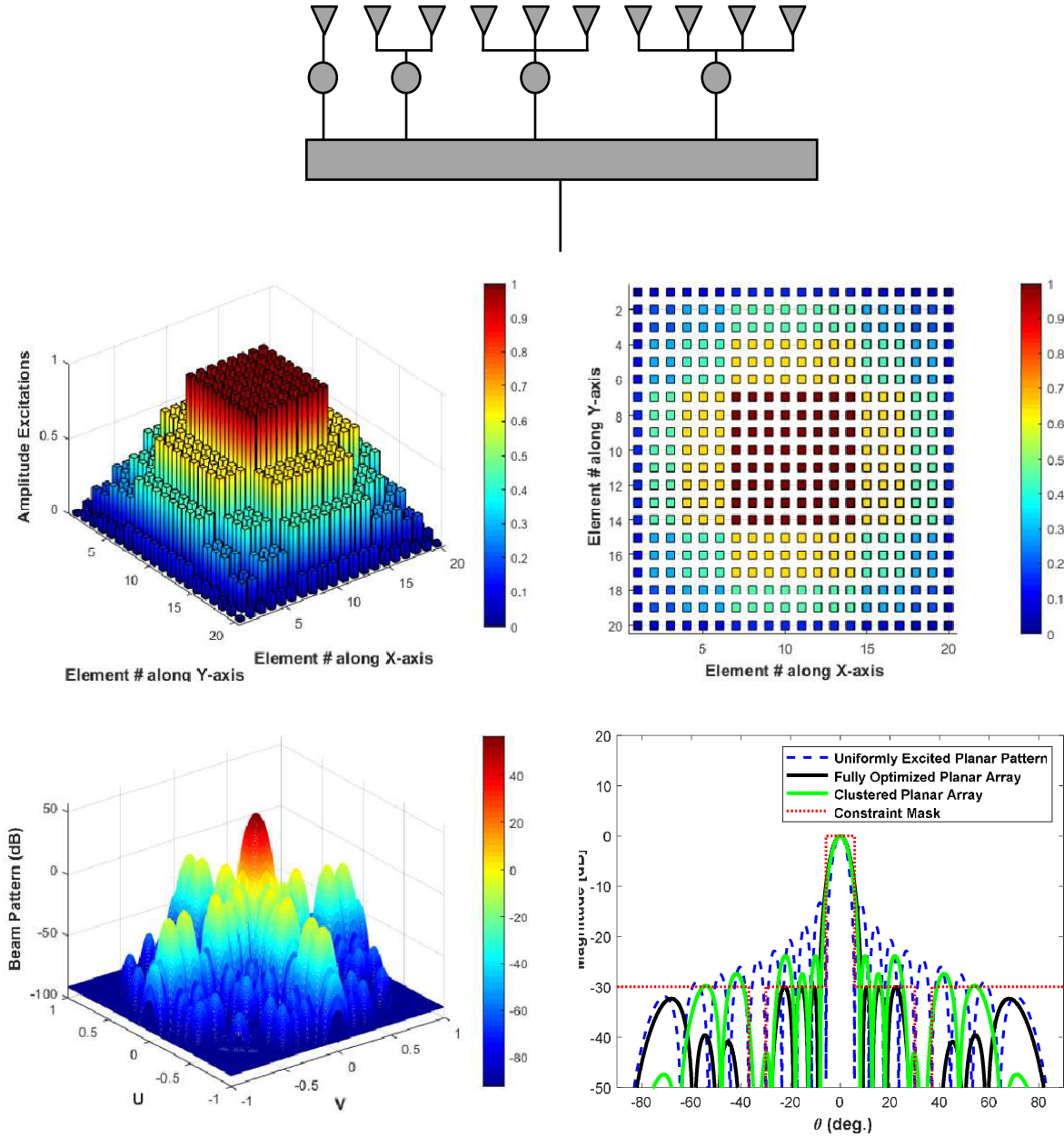


Figure 7. The results for incremental case for $E = 20$, $M = 8$ and unequal cluster sizes.

Table 2. Array performances for $E = 20$ linear array elements with incremental number of elements in each cluster.

	Performance	Distribution of Elements per Subarray							
		1	2	3	4	4	3	2	1
Subarray with Incremental Case	Complexity Reduction	60%							
	Taper Efficiency	0.9029							
	Directivity (dB)	25.7201							
	Peak SLL (dB)	-25							
	Average SLL (dB)	-21.84							
	FNBW (deg.)	6.58							

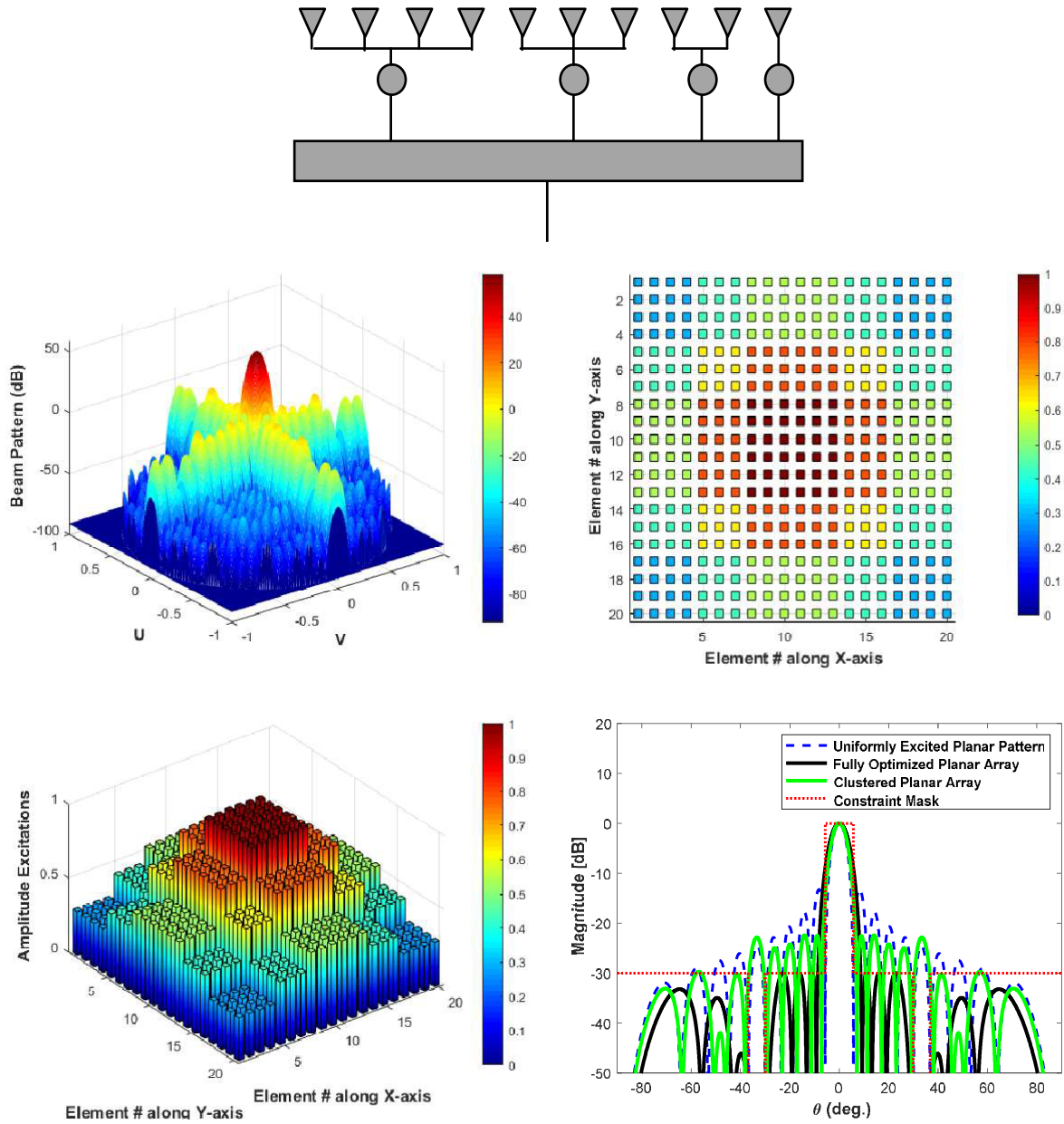


Figure 8. The results for decreasing case for $E = 20$, $M = 8$ and unequal cluster sizes.

Table 3. Array performances for $E = 20$ linear array elements with decreasing number of elements in each cluster.

	Performance	Distribution of Elements per Subarray							
		4	3	2	1	1	2	3	4
Subarray with Decreasing Case	Complexity Reduction (%)	60							
	Taper Efficiency	0.8201							
	Directivity (dB)	25.6652							
	Peak SLL (dB)	-22							
	Average SLL (dB)	-21.4816							
	FNBW (deg.)	6.6696							

until approaching the center of the array. Fig. 8 shows the proposed clustered array configuration and its results, while Table 3 shows its performance measures. From these results, it can be found that the peak SLL of this case is -22 dB which is higher than that of the allowable constraint level -30 dB and its capability to place the two wide nulls at $\pm 35^\circ$ as a previous design is found to be unsatisfactory.

5. CONCLUSIONS

Clustered amplitude tapering is highly desirable if grating lobes were not presented in the array pattern. In this paper, it is shown that the proposed method allows designers to use amplitude taper at the subarray level instead of its element level counterpart to simultaneously minimize the grating lobes and the sidelobes. Thus, lesser number of RF components is needed to implement such feeding network. Many clustered configurations have been investigated and their performances highlighted. For example, when an array is considered with the total number of elements, $E = 20$, number of clusters, $M = 4$, number of elements per cluster, $N_s = 5$, the complexity reduction is 80%, peak SLL = -19.15 dB, directivity = 26.32 dB, and taper efficiency = 0.91 . These results fully confirm the effectiveness of the clustered array. The method can be further extended to the concentric ring arrays where each cluster may be formed as a ring around the center of the array. Then, the number of elements per clustered ring may be increased/decreased as they approach the edges of the array. The amplitude tapers of the clustered rings as well as the clustered sizes may be both optimized to get the desired array pattern. This is left for another research work.

REFERENCES

1. Mohammed, J. R., "Synthesizing sum and difference patterns with low complexity feeding network by sharing element excitations," *International Journal of Antennas and Propagation*, Vol. 2017, Article ID 2563901, 7 pages, 2017.
2. Mohammed, J. R., "Obtaining wide steered nulls in linear array patterns by controlling the locations of two edge elements," *AEÜ International Journal of Electronics and Communications*, Vol. 101, 145–151, Mar. 2019.
3. Mohammed, J. R. and K. H. Sayidmarie, "Synthesizing asymmetric sidelobe pattern with steered nulling in non-uniformly excited linear arrays by controlling edge elements," *International Journal of Antennas and Propagation*, Vol. 2017, Article ID 9293031, 8 pages, 2017.
4. Holden, J. M., "Grating lobe minimization in sum and difference beam patterns," *IEEE International Symposium on Antennas and Propagation Society*, Vol. 1, 772–775, Jun. 22–27, 2003.
5. Haupt, R., "Reducing grating lobes due to subarray amplitude tapering," *IEEE Transactions on Antennas and Propagation*, Vol. 33, No. 8, 846–850, Aug. 1985.
6. Brockett, T. J. and Y. Rahmat-Samii, "Subarray design diagnostics for the suppression of undesirable grating lobes," *IEEE Transactions on Antennas and Propagation*, Vol. 60, No. 3, 1373–1380, Mar. 2012.
7. Jeong, T., J. Yun, K. Oh, J. Kim, D. W. Woo, and K. C. Hwang, "Shape and weighting optimization of a subarray for a mm-Wave phased array antenna," *Appl. Sci.*, Vol. 11, 6803, 2021, <https://doi.org/10.3390/app11156803>.
8. Nickel, U., "Subarray configurations for digital beamforming with low sidelobes and adaptive interference suppression," *Proceedings of IEEE International Conference on Radar, Alexandria*, 714–719, USA, 1995.
9. Tarran, C., M. Mitchell, and R. Howard, "Wideband phased array radar with digital adaptive beamforming," *High Resolution Radar and Sonar (Ref. No. 1999/051)*, 1/1–1/7, IEE Colloquium, May 11, 1999.
10. Manica, L., P. Rocca, and A. Massa, "Design of subarrayed linear and planar array antennas with SLL control based on an excitation matching approach," *IEEE Transactions on Antennas and Propagation*, Vol. 57, No. 6, 1684–1691, Jun. 2009.

11. Rocca, P., L. Manica, R. Azaro, and A. Massa, "A hybrid approach for the synthesis of sub-arrayed monopulse linear arrays," *IEEE Transactions on Antennas and Propagation*, Vol. 57, No. 1, 280–283, Jan. 2009.
12. Mailloux, R. J., S. G. Santarelli, T. M. Roberts, and D. Luu, "Irregular polyomino-shaped subarrays for space-based active arrays," *International Journal of Antennas and Propagation*, Vol. 2009, 1–9, 2009.
13. Abdulqader, A. J., J. R. Mohammed, and R. H. Thaher, "Antenna pattern optimization via clustered arrays," *Progress In Electromagnetics Research M*, Vol. 95, 177–187, 2020.
14. Haupt, R., "Optimized weighting of uniform subarrays of unequal sizes," *IEEE Transactions on Antennas and Propagation*, Vol. 55, No. 4, 1207–1210, 2007.
15. Mohammed, J. R., "A method for thinning useless elements in the planar antenna arrays," *Progress In Electromagnetics Research Letters*, Vol. 97, 105–113, 2021.
16. Keizer, W. P. M., "Linear array thinning using iterative FFT techniques," *IEEE Transactions on Antennas and Propagation*, Vol. 56, No. 8, 2757–2760, 2008.
17. Mohammed, J. R., "Thinning a subset of selected elements for null steering using binary genetic algorithm," *Progress In Electromagnetics Research M*, Vol. 67, 147–157, 2018.
18. Rodriguez, A., L. Landesa, J. L. Rodriguez, F. Obelleiro, F. Ares, and A. Garcia-Pino, "Pattern synthesis of array antennas with arbitrary elements by simulated annealing and adaptive array theory," *Microwave and Optical Technology Letters*, Vol. 20, No. 1, 48–50, Jan. 5, 1999.
19. Lopez, P. and J. A. Rodriguez, "Subarray weighting for the difference patterns of monopulse antennas: Joint optimization of subarray configurations and weights," *IEEE Transactions on Antennas and Propagation*, Vol. 49, No. 11, 1606–1608, Nov. 2001.
20. Mohammed, J. R., A. J. Abdulqader, and R. H. Thaher, "Array pattern recovery under amplitude excitation errors using clustered elements," *Progress In Electromagnetics Research M*, Vol. 98, 183–192, 2020.
21. Balanis, C. A., *Antenna Theory, Analysis and Design*, 4th Edition, Wiley, 2016.